Deepening of PRTF notches by selective modification of pinna surface reflection coefficient*

○ Parham MOKHTARI, Yutaro HIROTA, Daisuke MORIKAWA
(Toyama Prefectural University)

1 Introduction

Auditory cues for human sound localization in the vertical dimension (e.g., elevation angle in the median plane) are primarily the first two peaks and notches of head-related transfer functions (HRTFs) [1]. As these cues are generated by acoustic reflections within the outer-ear (pinna) cavities, they are essentially the same as the peaks and notches of pinna-related transfer functions (PRTFs). In the median plane, typically the peak frequencies are invariant while the notches vary with elevation angle [2].

Previous research has shown that broadband sounds delivered by headphones or tube-phones can be correctly externalized in front, provided the listener's peaks and notches are not overly smoothed [3], or a typical mean depth of the first two notches is either maintained or deepened [4]. In our experience with measurement/simulation of a range of pinnae, notches are not always deep and clearly defined at all elevation angles. An intriguing question then arises whether artificially deepening notches where they are not already clearly defined, may help enhance a listener's sound localization or spatial hearing in general.

With this motivation, we are interested in how the notches depend on pinna surface reflection or shape. Previously, we used acoustic simulation to calculate shifts in the first notch's frequency and amplitude in response to local (2 mm) changes in pinna surface reflection coefficient k_r [5]. Here, we extend that work by varying k_r jointly at multiple pinna-surface elements chosen carefully based on a prior sensitivity analysis, and observing the effect on the notch depth. Our research question is therefore whether, and to what extent, a notch can be deepened by judicious tuning of pinna surface reflection.

2 Baseline Simulation

An MRI-measured & voxelated right ear's [6] PRTF at a front location 1 m from the head center was calculated by 3D finite-difference time domain (FDTD) simulation with grid resolution 2 mm. The Kirchhoff-Helmholtz method was used to project the sound field around the pinna to the farfield observation point [7]. Sound speed c and medium density ρ at each voxel were set to values for either air or water; the baseline reflection coefficient at the air-pinna interface was thus $k_r = 0.999$. The peaks and notches of the calculated baseline PRTF (black curve in Fig. 2) are listed in Table 1.

Table 1 Baseline PRTF peak (P) and notch (N) frequencies (F) and gain amplitudes (A)

	P1	N1	N2	P2	N3	P3
F (Hz)	3860	7378	9116	10243	11054	13222
A (dB)	+14.5	-22.2	-19.6	+2.1	-14.0	+11.4

3 Single-Voxel Perturbations

Keeping the same pinna shape, c and ρ at each of the 1786 surface-voxels were modified one voxel at a time such that $k_r = 0.5$ at only that part of the surface, and each time the PRTF at 1 m in front was calculated. N1 frequency and amplitude were extracted on each PRTF and the baseline values were subtracted to obtain ΔF and ΔA. The 1786 pairs of deviations thus obtained are shown as a scatterplot in Fig. 1(a). The pinna sensitivity map for ΔA of N1 for the same data was shown previously (Fig.2(a) in [5]).

4 Multi-Voxel Perturbations

Next, a subset of surface voxels was selected, with the aim of deepening N1 while minimizing any effect on its frequency. Although there may be many possible ways to make such a selection, we simply defined a parabola $\Delta A =$

* 一部の耳介表面反射係数の選択的変更による PRTF ノッチの深化
モクタリ パーハム, 廣田 裕太郎, 森川 大輔 (富山県立大学)

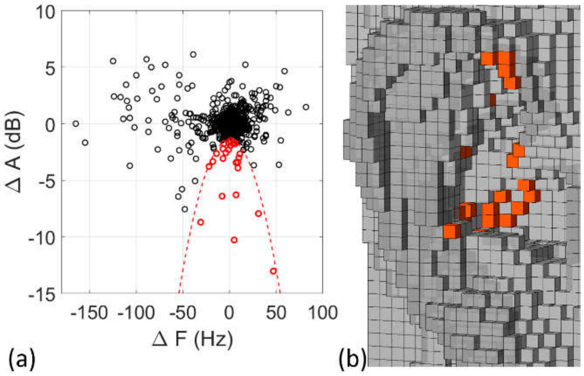

Fig. 1 (a) Effect of single-voxel perturbations on N1 frequency and amplitude, and the 26 voxels selected by a parabola (red); (b) a 3D view of the pinna highlighting the 26 selected voxels.

$-0.0046(\Delta F)^2 - 1.4$ on the scatterplot of Fig. 1(a), and chose all voxels that lay below the curve. The 26 voxels thus selected on the basis of their individual effects on N1, are colored on the pinna shown in Fig. 1(b).

Properties c and ρ at these 26 voxels were then jointly modified, such that k_r at only those parts of the pinna surface would be 0.5 as with the single-voxel perturbations. However, the resulting PRTF (dashed curve in Figs. 2 & 3) had a much shallower N1 and N2. Therefore, we modified the 26 voxels more subtly, such that k_r would be gradually reduced in the following 8 steps: 0.97, 0.95, 0.94, 0.93, 0.92, 0.91, 0.89, and 0.87.

The resulting PRTFs up to 15 kHz are shown in Fig. 2, and Fig. 3 shows an expanded view around N1 & N2 separately. In Figs. 2 & 3, the baseline PRTF is in black, the PRTFs for the 8 steps listed above are in various shades of blue, and red highlights the PRTF at $k_r = 0.93$, which attained the deepest N1 & N2. As the 26 selected voxels' k_r was reduced from 0.999 to 0.93, N1 and N2 sharpened and their amplitudes monotonically decreased, N1 reaching −53.6 dB and N2 reaching −61.7 dB. At the deepest levels, N1 frequency shifted from the baseline by only −70 Hz (i.e., by < 1 %), and N2 frequency shifted by only +2 Hz; thus, as intended in the voxel selection, notch frequencies were relatively unaffected. Further reduction of k_r below 0.93 gradually broadened and shallowed the notches. Meanwhile, the perturbations had almost no influence on the PRTF's peaks and notches at other frequencies.

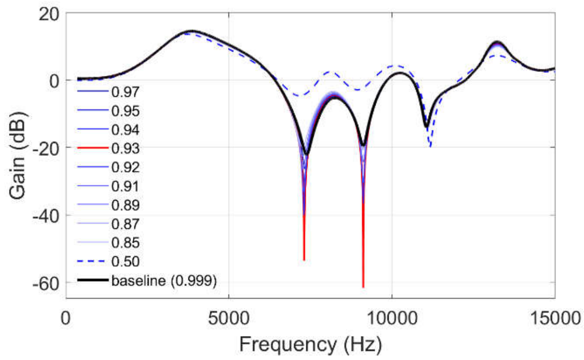

Fig. 2 Calculated PRTFs at 1 m in front. Black: baseline condition. Various blue: k_r at the 26 selected voxels reduced in steps. Red: deepest N1 and N2 at $k_r = 0.93$.

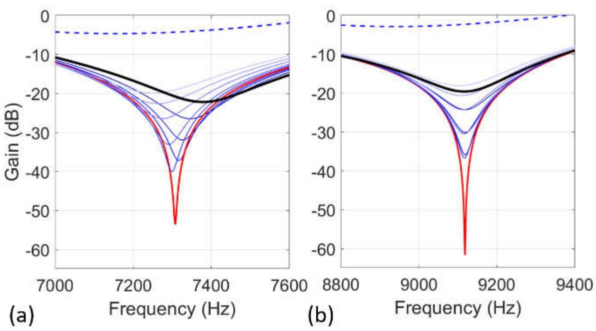

Fig. 3 Same as Fig. 2, zoomed in on N1 & N2.

5 Conclusions

A method was presented that, in principle, can deepen a PRTF's first two notches. Future work includes understanding the significance of the selected pinna-surface voxels in terms of the notch generation mechanism, extending the method to more than one farfield location, and investigating the auditory-perceptual effects of such modifications.

Acknowledgements

This work was partially supported by JSPS KAKENHI Grant Number JP17K00260.

References

[1] Iida & Ishii, Appl. Acoust. **129**, 239-247, 2018.
[2] Takemoto *et al.*, JASA **132**, 3832-3841, 2012.
[3] Kulkarni & Colburn, Nature, 747-749, 1998.
[4] Nishiyama & Iida, Proc.ASJ-Aut., 661-664, 2021.
[5] Hirota *et al.*, Proc.ASJ-Aut., 651-652, 2021.
[6] Hirahara *et al.*, Fundam. Review **2**, 68-85, 2009.
[7] Mokhtari *et al.*, Proc.ASJ-Aut., 611-614, 2008.